

Fallout of Lead over Paris from the 2019 Notre-Dame Cathedral Fire

Alexander van Geen ¹, Yuling Yao ², Tyler Ellis ¹, and Andrew Gelman ²

¹Lamont-Doherty Earth Observatory of Columbia University. Palisades, NY 10964, USA.

²Department of Statistics, Columbia University. New York, NY 10027, USA.

Key Points:

- Surface soil Pb concentrations within 1 km of Notre-Dame cathedral are about 200 mg/kg higher downwind of the fire relative to background.
- The corresponding fallout of 1000 kg Pb is 6 times higher than the estimated mass of Pb from the fire transported by the wind beyond 1 km.
- The resulting human exposure was probably dwarfed by the impact of leaded-gasoline in previous decades but warranted more testing sooner.

Corresponding author: Alexander van Geen, avangeen@ldeo.columbia.edu

Abstract

The roof and spire of Notre-Dame cathedral in Paris that caught fire and collapsed on April 15, 2019, were covered with 460 tons of lead (Pb). Government reports documented Pb deposition immediately downwind of the cathedral and a 20-fold increase in airborne Pb concentrations at a distance of 50 km in the aftermath. For this study, we collected 100 samples of surface soil from tree pits, parks, and other locations in all directions within 1 km of the cathedral. Concentrations of Pb measured by X-ray fluorescence range from 30 to 9000 mg/kg across the area, with a higher proportion of elevated concentrations to the northwest of the cathedral, in the direction of the wind prevailing during the fire. By integrating these observations with a Gaussian process regression model, we estimate that the average concentration of Pb in surface soil downwind of the cathedral is 430 (95% interval, 300-590) mg/kg, nearly double the average Pb concentration in the other directions of 240 (95% interval, 170-320) mg/kg. The difference corresponds to an integrated excess Pb inventory within a 1 km radius of 1.0 (95% interval, 0.5-1.5) tons, about 0.2% of all the Pb covering the roof and spire. This is over 6 times the estimated amount of Pb deposited downwind 1-50 km from the cathedral. To what extent the concentrated fallout within 1 km documented here temporarily exposed the downwind population to Pb is difficult to confirm independently because too few soil, dust, and blood samples were collected immediately after the fire.

Plain Language Summary

This study estimates the extent to which the population of Paris was exposed to lead as a result of the Notre-Dame cathedral fire of April 15, 2019. The concern stems from the large quantity of lead that covered the cathedral, some of which was injected into the air by the fire for several hours. In order to evaluate how much lead rising from the fire was redeposited nearby, surface soil samples were collected in all directions from tree pits and parks within a 1 km radius of the cathedral. Elevated levels of lead observed downwind of the cathedral indicate that surface soil preserved the mark of lead fallout from the fire. Although the estimated amount of lead redeposited within 1 km corresponds to only a small fraction of the total covering the cathedral, it could have posed a health hazard to children located downwind for a limited amount of time. Environmental testing on a larger scale immediately after the fire could have provided a more timely assessment of the scale of the problem and resulted in more pointed advice to the surrounding population on how to limit exposure to the fallout of lead.

1 Introduction

The roof and spire of Notre-Dame cathedral in the center of Paris covered with 460 tons of lead (Pb) tiles burned down within a few hours of a fire that started early on the evening of April 15, 2019, and took 9 hours for the fire brigade to extinguish (INERIS, 2019). The yellow color of the smoke rising from the cathedral during the first few hours has been attributed to PbO particles entrained with the hot ascending air and formed by heating to 600°C the lead on top of the vault of the cathedral. Prevailing winds combined with modeling of the plume of smoke particles rising from the fire have linked this increase to the ejection of about 150 kg of Pb, only 0.03% of the total covering the cathedral, into the atmosphere by the fire and redeposition over several tens of kilometers. This is consistent with observations at an air quality monitoring station 50 km downwind of the burning cathedral where a 20-fold increase in particulate Pb concentration, from 0.050 to 0.105 $\mu\text{g}/\text{m}^3$, was recorded during the week that followed the fire (Fig. 1a). The same INERIS (2019) report also states that considerably more Pb was likely deposited in the immediate vicinity of the cathedral but there was no attempt to estimate this amount.

The sequence of announcements and measures taken after the fire by local authorities provide a context for and contribute to the interpretation of the new Pb measure-

ments presented here. The consequences of the Notre-Dame fire are worth documenting because lead has neurotoxic effects even at low levels of exposure at a young age (Lanphear et al., 2005; Laidlaw and Filippelli, 2008; Aizer and Currie, 2019). Dust and soil are also known sources of child Pb exposure, including in France (Etchevers et al., 2015; Glorennec et al., 2016). Four days after the fire, on April 19th, the environmental non-governmental organization Robin des Bois (2019) issued a press release expressing concern about the likely large quantities of Pb mobilized by the fire, referring to potential health risks incurred by firefighters, workers on the site, and the surrounding population. On April 27th, almost two weeks after the fire, the Agence Régionale de la Santé (ARS, 2019a) co-issued a press release indicating that dust sampling had revealed some locally elevated levels of Pb and that areas very close to the cathedral that could not rapidly be cleaned had been closed to the public. The press release also recommended that nearby inhabitants remove indoor dust with wet wipes and announced follow-up studies to minimize risks to workers on the site and the surrounding population. On May 9, 2019, the ARS (2019b) confirmed soil Pb levels of 10,000-20,000 mg/kg in the out-of-bounds area very near the cathedral but also reported that no levels above 300 mg/kg, the maximum level recommended in France (HCSP, 2014), were measured outside this area within the Île de la Cité, where the cathedral is located. The same news release from the ARS reported that no sample collected around the cathedral to assess air quality exceeded the regulatory level of $0.25 \mu\text{g}/\text{m}^3$ for Pb in airborne particulate matter. This indicated that exposure through inhalation was unlikely, although the timing of the sampling relative to the fire was not provided.

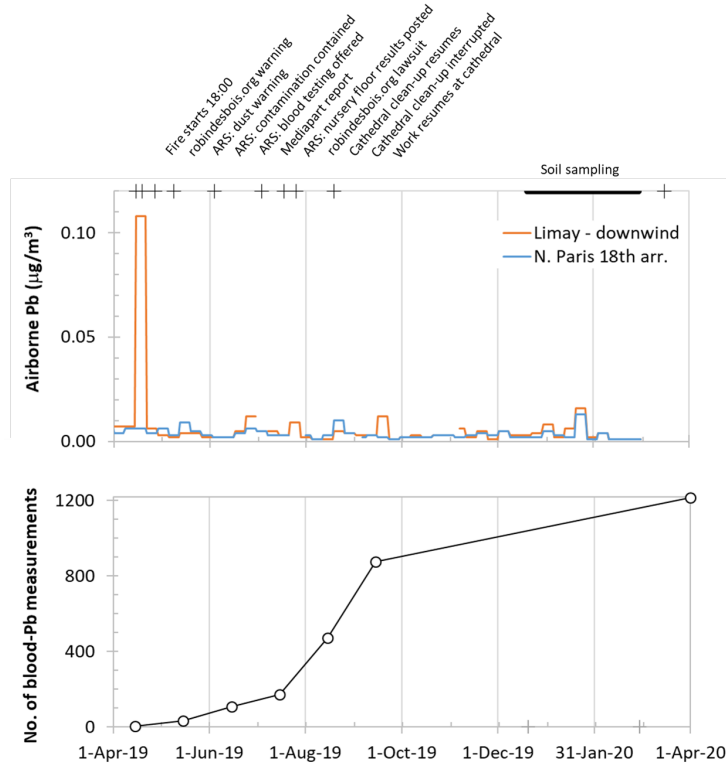


Figure 1: Events following the April 15, 2019 Notre-Dame cathedral fire shown with (a) weekly time series of Pb concentrations in airborne particulate matter measured at two Airparif monitoring stations (<https://www.airparif.asso.fr/en/>) and (b) the total number of children and adolescents in the 1st, 4th, 5th, and 6th arrondissements whose blood was tested for Pb (ARS, 2019g, h).

Almost a month later, on June 4th, the ARS (2019c) reported that indoor dust collected in some nearby apartments was found to be elevated in Pb and referred to a first child whose blood-Pb content was over 50 $\mu\text{g/L}$, the local intervention level requiring a follow-up investigation at home (HCSP, 2014). In the same press release, whose overall tone was meant to be reassuring, the ARS offered to test the blood of any children less than 7 years old residing on the Île de la Cité for Pb at a nearby hospital. On July 18, 2019, the ARS (2019d) issued a 100+ page report indicating no blood-Pb levels above 50 $\mu\text{g/L}$ had been detected in 81 children from the 1st, 4th, 5th, and 6th arrondissements, all areas downwind of the fire, and that a Pb source unrelated to the fire was identified in the home of the previously reported child with $>50 \mu\text{g/L}$ Pb in blood. The same document indicated that indoor surface Pb concentrations at a number of nurseries sampled downwind of the fire were all $<1000 \mu\text{g/m}^2$, the local regulatory level after lead remediation in housing, and mostly $<70 \mu\text{g/m}^2$, the level above which a blood test is encouraged (HCSP 2014), along with a detailed map of measurements of Pb concentrations in surface dust of the area. Unlike soil measurements, which require unconsolidated material such as a tree pit or a park, surface Pb measurements, usually conducted indoor, rely on wiping a hard surface (e.g. a sidewalk) over a set area with a wet tissue that is then analyzed. This is a standard regulatory procedure in France as well as in the U.S. (Lanphear et al., 1995; JORF, 2009).

On July 26, Robin des Bois filed a lawsuit claiming insufficient measures were taken to protect the health of workers on the cathedral site, after which activities were interrupted for several weeks (Le Monde, 2019). Soon thereafter on August 4, the ARS (2019e) tried to refute allegations by Mediapart (2019), an investigative online news provider, that it was minimizing the risk of Pb exposure to the population residing downwind of the cathedral. On November 27, however, the ARS (2019f) announced online access to georeferenced environmental Pb data collected both before and after the cathedral fire (<https://santegraphie.fr/mviewer/?config=app/notredame.od.xml>). The data posted by the ARS include a dozen wipe-based surface Pb measurements conducted in 2018 in close proximity to the cathedral and about 60 measurements of the same type in the same area from 2020. In the 2018 and 2020 data, only one measurement exceeds 5000 $\mu\text{g/m}^2$ Pb, and this by less than a factor of two.

For 2019, the database contains a much larger number of measurements around the cathedral, including dozens extending over a distance of 50 km in the direction of the plume and the air-quality monitoring station of Limay where an increase in airborne Pb had been detected during the week after the fire (Fig. 1). Outside a radius of 2 km from the cathedral, none of the reported measurements exceed 5000 $\mu\text{g/m}^2$. Between 1 and 2 km from the cathedral, a subset of 7 out of a total of ~ 40 measurements, all conducted between mid-May and mid-June 2019, exceed 5000 $\mu\text{g/m}^2$ and but in all but one case by less than a factor of 10. Within a radius of 1 km of the cathedral, the proportion and level of elevated surface Pb measurements is comparable to the findings in the 1-2 km range, although the majority of these measurements date from summer and fall 2019, i.e. several months later. It is only within a radius of 100 m from the cathedral that much higher surface Pb concentrations, most over 100,000 $\mu\text{g/m}^2$ and several near 1,000,000 $\mu\text{g/m}^2$ are reported on the ARS site.

The ARS georeferenced data site only lists 24 soil Pb measurements within a radius of 2 km from the cathedral, all conducted after the fire and between April and June 2019. Most of the reported Pb concentrations are below 100 mg/kg, with 6 in the 100-300 mg/kg range, and only one higher value of 310 mg/kg within 100 m of the cathedral. These values do not seem consistent with the 10,000-20,000 mg/kg concentrations reported for the same area by the ARS (2019b), which were not posted, unless the measurements were obtained by different methods. The soil protocol followed by the ARS calls for sampling to 5 cm depth and homogenizing this material before analysis. In the case of Pb contamination limited to the top 1 mm, this could lead to >50 -fold lower con-

centrations than measured from the very surface with a hand-held XRF fluorescence analyzer (Landes et al, 2019). Diluting the highest reported surface Pb concentration of 1,000,000 $\mu\text{g}/\text{m}^2$ over the mass of soil to 5 cm depth would, for instance, increase the soil Pb concentration by only 10 mg/kg, i.e. little more than 10% of background levels based on the other measurements. The relatively low soil concentrations posted on the ARS site are therefore not necessarily inconsistent with the much higher levels referred to in the earlier press release.

One of the goals of this study was to determine if a very basic soil sampling procedure of the fallout paired with more advanced statistical analysis could yield useful information. Provided sampling is limited to the top ~ 1 cm, soil has the advantage of preserving the signal of a fallout for much longer than hard surfaces such as road and sidewalks that are swept by wind and flushed by rain. Our surface soil data collected 9-10 months after the fire show that the population residing within 1 km and downwind of the fire was probably considerably more exposed to Pb fallout, albeit for a brief period, than indicated by measurements and surveys conducted by local authorities weeks to months later. The study demonstrates that the public should expect data to be collected and offered to scrutiny immediately after an environmental accident. Besides knowing where a potential hazard is located, posting of data creates incentives for local authorities to act transparently and in the public interest. Other cases, albeit of a very different magnitude, where lack of data unnecessarily diminished public trust and may have led to the wrong official responses include the nuclear reactor accidents in Chernobyl and Fukushima (Alexievich, S., 2006; Brown et al., 2016).

2 Materials and Methods

2.1 Data collection

One hundred soil samples were collected between December 20, 2019 and February 29, 2020 mostly from tree pits (55 samples) and parks or smaller garden-like areas (30). In a few cases, samples were collected from small gaps in the sidewalk (13) or even semi-permanent plant pots (2) for lack of more suitable alternatives. One set of 58 soil samples were spaced roughly equally along two concentric circles of 400 and 1000 m in radius centered on the cathedral (Fig. 2). The remaining 42 samples targeted the area likely to have been impacted by fallout from fire, downwind of the cathedral.

A large metal spoon was used to recover ~ 50 g of material from the upper ~ 1 cm of each site. The samples were dried overnight in paper bags, after which the fine fraction was separated through a metal kitchen sieve (~ 1 mm mesh size) and poured into 20 mL scintillation vials. Without further processing, the fine fraction was analyzed in the inverted vials through plastic cling wrap using a handheld Innov-X (now Olympus) Delta Premium X-ray fluorescence analyzer. The XRF's internal calibration was confirmed by bookending both rounds of analyses with Standard Reference Material soil 2711a from the US National Institute of Standards and Technology. The average of $1,480 \pm 40$ mg/kg ($n = 4$) obtained for Pb was consistent with the certified value of 1400 ± 10 mg/kg.

The XRF measures the concentrations of 16 additional elements. Tin (Sn) is of particular interest for the present study but there is no certified Sn value for SRM 2711a. Landes (2019) compared soil Sn concentrations measured by the same instrument with two dozen soil digests analyzed by inductively-coupled plasma mass spectrometry (Cheng et al., 2004). The slope of Sn concentrations measured by XRF as a function of concentrations measured by ICPMS of 1.64 indicates a systematic overestimate of Sn concentrations by XRF.

Soil Pb concentrations are also displayed in a polar coordinate centered on the cathedral to help to visualize the impact of the fire independently of the presumed direction



Figure 2: Map of 100 soil sample locations around the cathedral and their Pb concentrations. The two circles of samples centered on the cathedral have radius of 400 and 1000 m, respectively. Additional samples were collected in downwind direction, northwest of the cathedral.

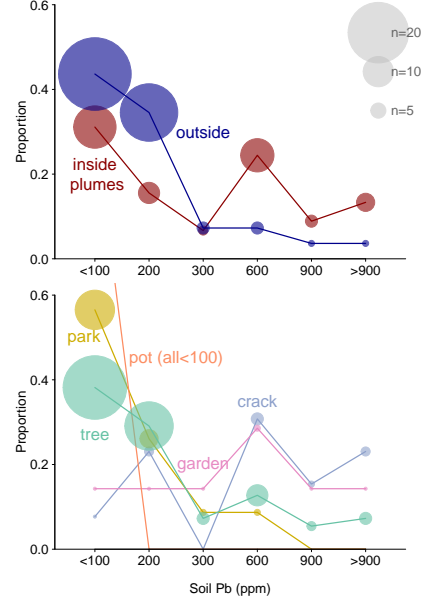


Figure 3: (a) Proportion of soil Pb collected inside and outside the area passed over by the plume of smoke rising from the cathedral. (b) Proportion of Pb sample for different types of soils. The size of the symbols indicates the number of samples in each grouping. The two plant pots are low in Pb and their symbol out of range.

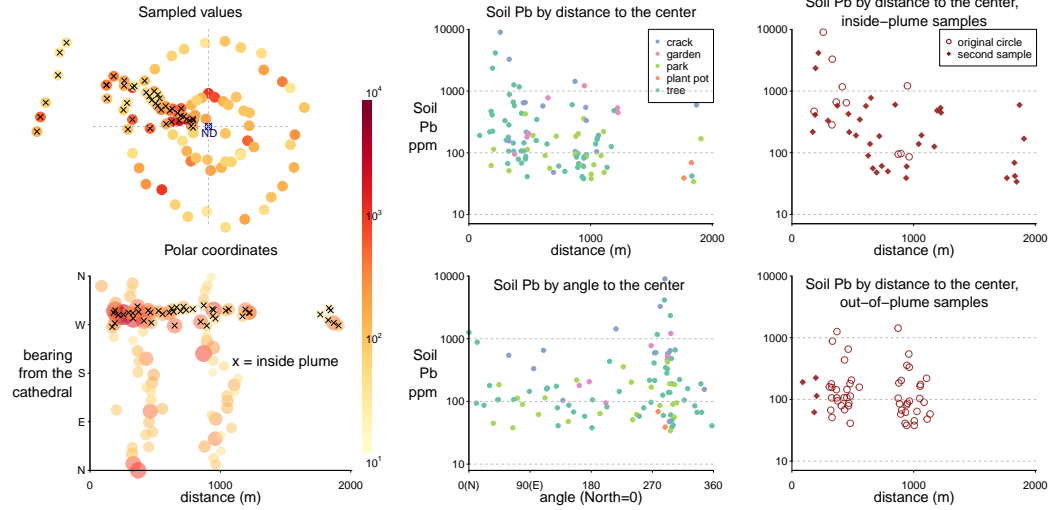


Figure 4: Left column: Sampled locations and Pb concentrations in both Cartesian and polar coordinates. Middle column: scatter plot of soil Pb by distance and bearing from the cathedral, colored by soil type. Right column: soil Pb by distance from the cathedral, grouped by inside/outside plume.

of the plume (Fig. 4). The sampled Pb peaks at the northwest, and as a whole, drops off with a longer radial distance, while the slope inside the plume is sharper. Based on INERIS (2019), we specify the plume region to be the sector between 260° to 310° clockwise from the cathedral (Fig. 4).

2.2 Notation and pre-processing

We denote the soil Pb concentration (in mg/kg) in the i -th location to be y_i , $i = 1, \dots, n$, and compute the its radial distance r_i (in km) and the bearing θ_i (in degrees, North = 0, East = 90) from the cathedral. We index the type of soil by $k[i] \in \{1, 2, \dots, 5\}$ to represent where the i -th sample was drawn from: cracks in the sidewalk, smaller garden areas, park, plant pots, or tree pits.

As for many other natural measurement, the observed y_i has a heavy right tail. Directly modeling y will often make the model sensitive to the few extreme values. Measurement errors in chemical analysis are often additive in the lower end and multiplicative in the high end. Therefore instead of a log transformation, we prefer a $1/4$ -th power transformation, as the measurement errors would likely be of similar order of magnitude in different sites. For notation simplicity, we will plug in $y^{1/4} \rightarrow y$ in the model description we use, and transform it back to the ordinary scale after model fitting.

The concentration of soil Pb varies both spatially and by soil type. We decompose the outcome y_i into three terms:

$$y_i = \mu_{k[i]} + f(r_i, \theta_i) + \epsilon_i, \quad \epsilon_i \sim N(0, \sigma^2), \quad i = 1, \dots, n.$$

which includes

- the soil type coefficient $\mu_{k[i]}$; it depends only on what type of soil the sample belongs to;
- the spatial term $f(r_i, \theta_i)$; it depends only on where the sample is collected (encoded by distance and bearing);
- an independent observational noise ϵ_i ; it contains measurement error, small-scale fluctuations, and effects from any unmeasured covariates.

2.3 Hierarchical modeling of different soil types

The lower row of Fig. 3 and the middle column of Fig. 4 suggest that the type of soil (tree pit, park, smaller garden areas, cracks in the sidewalk, plant pots) is predictive of Pb concentrations. The sample sizes in different types are unbalanced, and a simple sample mean is noisy for groups with small samples. To partially pool across the data, we fit a hierarchical model to the soil type coefficients μ_k .

However the model is not identifiable yet, as a additive constant can be extracted from the μ and added to f . To resolve this, we restrict the soil-type coefficients by a zero-sum constraint, $\sum_{k=1}^5 \mu_k = 0$.

2.4 Modeling the Pb distribution by a Gaussian process regression

We model the spatial pattern nonparametrically by placing a mean-zero Gaussian process prior on the latent function f . It models the joint distribution at any two locations, $f(r, \theta), f(r', \theta')$, using a multivariate Gaussian distribution. To flexibly account for the influence from the distance, bearing, and their interactions, we use a product kernel in the Gaussian process prior:

$$K(r_1, \theta_1, r_2, \theta_2) := \text{Cov}(f(r_1, \theta_1), f(r_2, \theta_2)) = \alpha K_1(r_1, r_2) K_2(\theta_1, \theta_2),$$

where for distances, we adopt the commonly-used squared exponential kernel:

$$K_1(r_1, r_2) = \exp \left(-\frac{(r_1 - r_2)^2}{\rho_r^2} \right).$$

For the bearing, we employ a periodic kernel:

$$K_2(\theta_1, \theta_2) = \exp \left(-\frac{2 \sin^2(\pi|\theta_1 - \theta_2|/360)}{\rho_\theta^2} \right).$$

Besides the soil type effect μ , spatial latent function f , and scale of the observational variation σ , the model also contains hyperparameters α : the scale of the spatial signal (how strong the spatial pattern is); ρ_d : the length scale in the distance dimension (how rigid the function f can change over distance); and ρ_θ : the length scale in the angle dimension.

Since the modeled outcome $y^{1/4}$ and the distance (in km) are all roughly unit-scaled, we adopt weakly informative priors

$$\rho_d \sim N(0, 1.5^2), \quad \rho_\theta \sim N(0, 1), \quad \alpha, \sigma \sim N(0, 6^2), \quad \mu_k \sim N(0, 1), \quad k = 1, \dots, 5.$$

We sample from the posterior distribution of all parameters in the model using Stan (Stan Development Team, 2018). In our example, the chains mixed well for 4 chains and 3000 iterations per chain.

2.5 Inference from the fitted model

2.5.1 Spatial imputation from the model

We sample a uniform 30×30 grid of locations $(\tilde{\rho}, \tilde{\theta})$ in the 1.5 km neighborhood. After integrating out the posterior distribution, we obtain the posterior predictive distribution of the outcome values at this location $\tilde{f} = f(\tilde{\rho}, \tilde{\theta})$ is from

$$\tilde{f} | \tilde{\rho}, \tilde{\theta}, \rho, \theta, f \sim N \left(K(\tilde{\rho}, \tilde{\theta}, \rho, \theta) K^{-1}(\rho, \theta) f, K(\tilde{\rho}, \tilde{\theta}) - K(\tilde{\rho}, \tilde{\theta}) K^{-1}(\rho, \theta) K(\rho, \theta, \tilde{\rho}, \tilde{\theta}) \right). \quad (1)$$

We model the outcome to the $1/4$ power and transform f back to f^4 in the visualizations.

Further, we add the observational noise and generate the posterior predictive distribution of \tilde{y} outcome \tilde{y} in location $(\tilde{\rho}, \tilde{\theta})$ by location $\tilde{f} = f(\tilde{\rho}, \tilde{\theta})$ is from

$$\tilde{y} | \tilde{f} \sim N(\tilde{f} | \sigma_{\text{sim}}^2), \quad \sigma_{\text{sim}} \sim p(\sigma | y). \quad (2)$$

This amount to the prediction of the outcome in a typical soil type with $\mu = 0$ such that we can make fair comparison of pure spatial effects in the later sections.

We do not impute locations with $\tilde{r} < 100$ m. We do not have any data in that region and any inference relies on extrapolation.

2.5.2 Excess Pb inside the plume

The plume is a cone defined by $\mathcal{C} = \{\theta : 260^\circ < \theta < 310^\circ\}$. At each distance \tilde{r} , we compute the plume excess, the difference of soil Pb (ppm) between the plumes on the outside along the radius r ring, by

$$\text{Excess}^f(\tilde{r}) = \frac{\sum_{j: \tilde{\theta}_j \in \mathcal{C}} f(\tilde{\theta}_j, \tilde{r})}{\sum_{j: \theta_j \in \mathcal{C}} 1} - \frac{\sum_{j: \tilde{\theta}_j \notin \mathcal{C}} f(\tilde{\theta}_j, \tilde{r})}{\sum_{j: \theta_j \notin \mathcal{C}} 1}, \quad (3)$$

where $f(\tilde{\theta}_j, \tilde{r})$ is a posterior predictive draw of \tilde{f} at location $\tilde{\theta}_j, \tilde{r}$ using (1). Because it is calculated using posterior draws, expression (3) is a random variable whose posterior distribution we can summarize using the mean or quantile of its simulation draws.

Likewise we compute the excess Pb at the observational level,

$$\text{Excess}^y(\tilde{r}) = \frac{\sum_{j:\tilde{\theta}_j \in \mathcal{C}} y(\tilde{\theta}_j, \tilde{r})}{\sum_{j:\tilde{\theta}_j \in \mathcal{C}} 1} - \frac{\sum_{j:\tilde{\theta}_j \notin \mathcal{C}} y(\tilde{\theta}_j, \tilde{r})}{\sum_{j:\tilde{\theta}_j \notin \mathcal{C}} 1}. \quad (4)$$

where $y(\tilde{\theta}_j, \tilde{r})$ denotes a posterior predictive draw of $\tilde{y}|\tilde{f}(\tilde{\theta}_j, \tilde{r})$ using (2). In general, $\text{Excess}^y(\tilde{r})$ has a larger posterior variance. It is because of the noise ϵ : such that there are more uncertainty even if we repeat sampling in the same location. It also has larger posterior mean than $\text{Excess}^f(\tilde{r})$. This is due to the multiplicative measurement error in ϵ . For example, if there is a multiplicative noise source that will halve or double the true value f with equal probability, the posterior mean of y becomes $\frac{2+0.5}{2}f = 1.25f$.

We further aggregate the the excess amount of Pb in the plume within the circle of radius r . To this end, we reweigh the excess density of the ring by its radius,

$$\text{Excess}_{\text{circle}}^f(\tilde{r}) = \int_0^{\tilde{r}} r' \text{Excess}^f(r') dr', \quad (5)$$

and

$$\text{Excess}_{\text{circle}}^y(\tilde{r}) = \int_0^{\tilde{r}} r' \text{Excess}^y(r') dr'. \quad (6)$$

Finally we estimate the excess amount of Pb of the plume inside a circle with any given radius r by

$$\frac{|\mathcal{C}|}{360} \times \pi \tilde{r}^2 \times \text{thickness} \times \text{soil density} \times \text{Excess}_{\text{circle}}^y(\tilde{r}). \quad (7)$$

For all the above quantities we compute the posterior mean, 50%, and 95% intervals using the simulation draws.

3 Results

3.1 Raw data summary

Concentrations of Pb measured in all surface soil samples range from 30 to 9,000 mg/kg and average 400 mg/kg (median of 140 mg/kg). All four Pb concentrations >2000 mg/kg are inside the plume area and within a distance of 400 m from the cathedral. Overall, soil Pb concentrations average 200 mg/kg outside ($n = 45$) and 400 mg/kg ($n = 55$) inside the plume area, respectively (Fig. 2). Average soil Pb for tree pits (300 mg/kg; $n = 55$) and garden areas (500 mg/kg; $n = 7$) are comparable, but markedly lower in park areas (130 mg/kg; $n = 23$). Cracks in the sidewalk (1400 mg/kg, $n = 13$) on the other hand are often higher in Pb than neighboring tree pits and garden areas (Fig. 3). Among the other soil constituents analyzed by XRF, only Sn shows a systematic relationship with Pb at higher concentrations. For 8 samples in the 1000-9000 mg/kg range of Pb concentrations, the mass ratio of Sn relative to Pb averages 3.5% after recalibrating the XRF signal.

Unlike air, water, and food, there is no standard in France for the Pb content of soil in outdoor public areas. A recommendation from French health authorities of 300 mg/kg corresponds approximately to the level at which blood-Pb of 5% of infants coming in contact with the soil would exceed a threshold of 50 $\mu\text{g/L}$ (HCSP, 2014). For comparison, the current US Environmental Protection Agency standard for residential soil

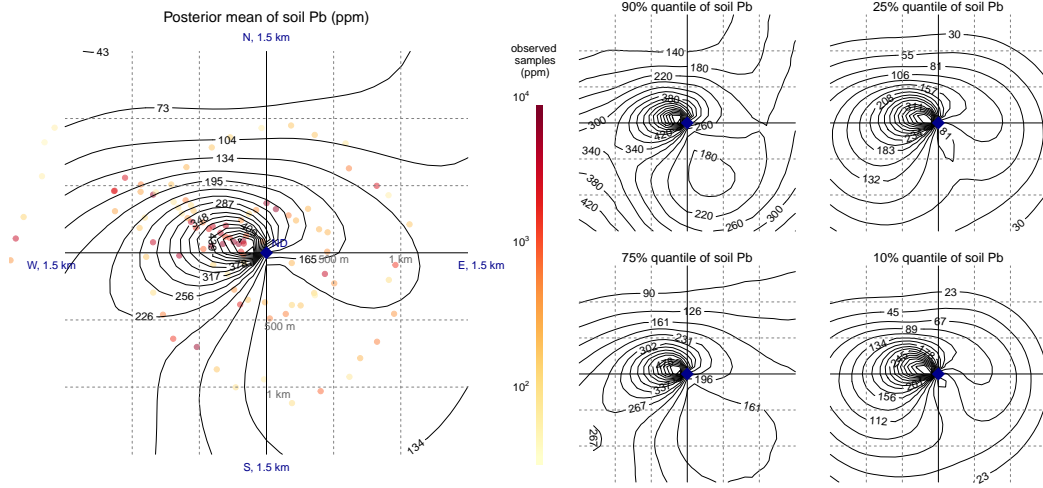


Figure 5: Contour plot of posterior mean and quantiles of \tilde{f} (net of soil types and measurement errors) of soil Pb concentrations within 1.5 km of the cathedral.

in areas where children play is 400 mg/kg Pb, but lowering this value is under discussion. Relative to 300 mg/kg, the Pb content of 29 of our 100 samples exceeds the French recommended value, 21 of which inside the plume area and 8 outside (Fig. 3). Considering only the samples collected along the two concentric circles to avoid bias, the average soil Pb content within the plume is 500 ± 200 mg/kg ($n = 7$, 1 sd), compared to 200 ± 40 mg/kg ($n=51$) outside the plume (Fig. 4).

3.2 Model inference

Contours of modeled Pb concentrations show more elevated levels in a northwesterly direction from the cathedral compared to other areas (Fig. 5). Although this peak was identified independently, it corresponds closely to the direction of the plume derived from meteorological observations (INERIS, 2019). Bayesian inference encodes all uncertainty, which is displayed as 90%, 75%, 25%, 10% quantiles of the predicted spatial concentration of soil Pb concentrations $f(\tilde{r}, \tilde{\theta})$, at all imputed locations among the 1.5 km neighborhood around the cathedral (Fig. 5). The estimation separates all measurement errors and soil types. In locations where not enough data is collected nearly (south, east), the model essentially has to extrapolate, but the posterior standard deviation of \tilde{f} is also large.

The effect of soil types indicates a decline in Pb concentrations from cracks in the sidewalk to tree pits and parks (Fig. 6). The effect of areas described as gardens is more variable, and poorly constrained in the two cases of the two plant pots. The number is on the scale of $y^1/4$, and for the median values $y \approx 140$, an additive effect of $0.5(-0.5)$ on $y^1/4$, which corresponds to $100(-65)$ ppm increase on y .

The model estimates Pb concentrations f as a function of the bearing from the cathedral, evaluated at distances of 400 m and 1000 m and average concentrations over all distances < 1.5 km (Fig. 7). At the 400 m ring, the soil Pb for outside-plume-average is about 190 (95% interval, 130-270) mg/kg, and peaks at 490 (95% interval, 330-710) mg/kg in the core of the plume.

The posterior predictive distribution of $\text{Excess}^f(\tilde{r})$ (Eqn. 3) shows that the difference in Pb concentration between inside and outside the plume declines from 350 (95%

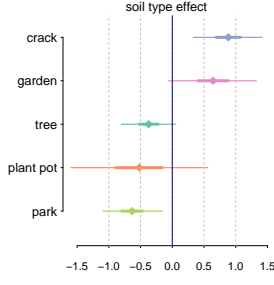


Figure 6: *Posterior mean, and 95% intervals for soil type effects μ_k .*

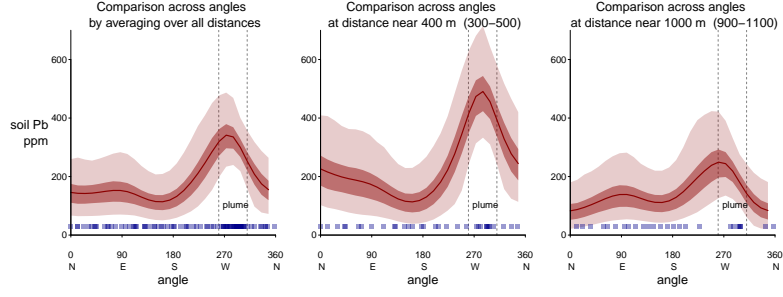


Figure 7: *Modeled Pb concentrations as a function of direction in relation to the cathedral, evaluated at distances of 400 m and 1000 m and averaged over all distances <1.5km.*

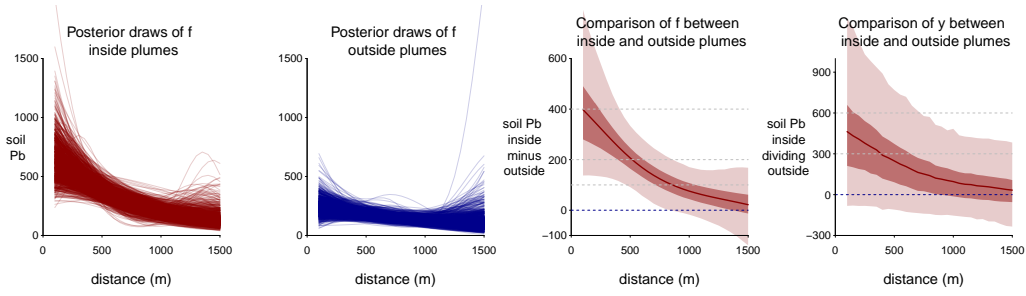


Figure 8: *From left, 1-2: Posterior draws of mean Pb concentrations \tilde{f} inside and outside plumes as a function of distance from the cathedral. The uncertainty is large small and large distance where there is no nearby data. 3: The posterior mean, of the difference between and inside and outside the plume (Eqn. 3). 4: The comparison of predicted Pb concentrations to be observed \tilde{y} (Eqn. 4). With additional observational noise added, the uncertainty interval is much wider.*

interval, 140-640) mg/kg at 200 m from the cathedral to 200 (95% interval, 90-330) mg/kg at 500 m, and 90 (95% interval, 0-190) mg/kg at 900 m, respectively, and vanishes beyond that distance (Fig. 8).

The model also calculates the average excess Pb inside a given radius (Eqn. 5–6) on both the mean response f and with additional observational noise respectively (Fig. 9). On the observational level y , inside the 1 km circle, the average concentration of Pb inside the plume is 430 (95% interval, 300-590) mg/kg is nearly double the average Pb concentration in the other directions of 240 (95% interval, 170-320) mg/kg. Finally, the model calculates the corresponding integrated mass of excess is 1.0 (95% interval, 0.5-1.5) metric tons of Pb at a 1000 m distance from the cathedral and becomes poorly constrained beyond that distance for lack of data (Fig. 9).

4 Discussion

Soil Pb concentrations around Notre-Dame cathedral show considerable spatial variability, both inside and outside the plume area. In some cases, this may reflect site-specific factors such as newly added soil (Fig. 6). This may be why park areas are generally lower in Pb. Cracks in the sidewalk, on the other hand, are generally higher in Pb possibly because of a preserved legacy of contamination from decades of leaded gasoline use. An oc-

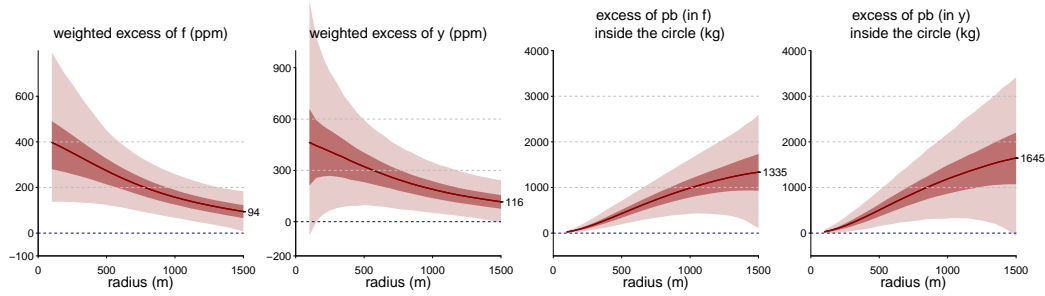


Figure 9: From left, 1-2: The average excess Pb (Eqn. 5–6) inside the radius- r -circle, of the mean response f and observation y . 3-4: The accumulated exceed Pb (Eqn. 7) inside the radius- r -circle.

casional highly local source of contamination from Pb paint or other sources cannot be ruled out, although these were apparently not sufficient to erase a pattern that is consistent with the trajectory of the plume. The model effectively subtracts systematic differences in background Pb concentrations for different soil types when calculating the excess inside the plume to outside the plume.

The Pb tiles covering the roof of the cathedral and the spire date to the second half of the 19th century (Daly, 1866). Some combination of Sn and Pb in solder was probably used extensively to cover the roof and spire of the cathedral. The relatively constant proportion of Sn relative to Pb in the soil with very high levels of Pb can therefore be attributed to the fire. Concentrations of Sn relative to Pb are not sufficiently elevated, however, to separate different sources of Pb at lower levels of contamination.

The background level below 200 mg/kg Pb outside the plume is plausible given average crustal Pb concentrations of <100 mg/kg with perhaps some legacy of leaded-gasoline use until 2000 (Miquel, 2001). Without the model, the difference in Pb concentrations between the area inside and outside the plume would have been poorly constrained (Fig. 8). A key question is the extent to which this excess is representative of the overall fall-out over the plume area, including hard surfaces such as sidewalks and roads where this excess could have been washed away by rain. Only 3 mm of rain was recorded during the week following the fire, but a total of 92 mm fell over Paris within 4 four weeks of the fire (<https://www.historique-meteo.net/france/ile-de-france/paris/2019/04/>).

Lead has a particularly strong tendency to adsorb to mineral surfaces (Selim, 2017). Once in contact with soil, Pb is therefore unlikely to be flushed off particles by water, especially within less than a year, unless by physical removal of the soil. If anything, tree pits might be concentrating Pb from a larger area if surface runoff percolates through tree pits and supplies particles from nearby hard surfaces. However, this also seems unlikely given the extensive drainage system along the sides of the streets of Paris, which is lower in elevation than the sampling sites.

A more likely mechanism for concentrating Pb in tree pits is capture of airborne particles by tree leaves, followed by rainfall rinsing the leaves or settling of the leaves into the tree pit. Studies of the natural radioisotope ^{210}Pb , whose atmospheric fallout is known, have shown that this process can enhance its accumulation by one- to two-thirds under the canopy of trees (Fowler et al., 2004), but not by an order of magnitude. Parks without trees, on the other hand, should not be subject to this process and might be more indicative of the fallout, at least in the short term and before erosion or the addition of new soil.

For comparison of our estimate of 1000 kg of excess Pb deposited downwind of the fire, the 50 km-long plume emanating from fire beyond a distance of 1 km was estimated to contain about 150 kg Pb on the basis of a furnace experiment using a combination metallic Pb and plastic (INERIS, 2019). Whereas the possibility of preferential accumulation of Pb in tree pits cannot be ruled out, the amount of Pb deposited within 1000 m of the cathedral estimated from the soil survey is fairly well constrained. About 6 times more Pb was therefore deposited within 100-1000 m of the cathedral than beyond that distance. For perspective, the addition of Pb to gasoline resulted in air emission of 4100 tons of Pb per year in France in 1990 (Miquel, 2001). Using population as a proxy for traffic and accounting for the one-fifth proportion of the French population residing in the greater Paris region, this suggests that the population of the city was exposed at the time to emissions of about 800 tons of Pb every year. Leaded gasoline was banned in 2000 and airborne emissions of Pb have dropped by at least an order of magnitude since Motelay-Massei et al. (2005). The impact of the Notre-Dame fire would therefore have been dwarfed by the impact of automobile traffic a few decades ago, and much harder to detect in soil.

A puzzle arises when the average excess of 200 ppm/kg Pb in the plume is converted, using our approximate sampling depth of 1 cm, to 4,000,000 $\mu\text{g}/\text{m}^2$ Pb, the unit and type of measurement more frequently referred to in regulation of indoor surfaces, including in schools. Such very high levels are reported on the interactive ARS map only within 100 m of the cathedral itself, in an area that was still out of bounds for the general public as of May 2020. At greater distances, but still within 1000 m of the cathedral, reported values are all below 20,000 $\mu\text{g}/\text{m}^2$. Many of the reported measurements, however, date from summer 2019 or later by which time much of the Pb fallout could have been flushed off hard surfaces such sidewalks and roadways by rain or washing. Even if our soil Pb measurements could overestimate the overall Pb fallout by a factor of 2 because of local concentration, it appears likely that the measurements based on outdoor surface wipes reported by the government considerably underestimate the amount of the Pb that was actually deposited in the plume area because of their timing. Concentrations of Pb on hard surfaces are likely to return more rapidly to background than in soil, whose retained inventory is therefore likely to provide a more accurate record of the fallout from the fire.

What are the implications of the soil-based findings for human exposure in the plume area in the aftermath of the fire, especially for small children who are most vulnerable? No children are likely to play around the tree pits themselves or even the sampling sites designated as gardens, many of which are not suitable playing areas (see interactive map with photos listed under the Acknowledgments). Fortunately, the more likely playing areas such as parks were generally low in Pb (Figs. 4, 6). The potential source of exposure therefore lies elsewhere and would have been the dust deposited during and immediately after the fire. This impact is difficult to ascertain independently for lack of specific information about in-house swipe measurements and a sufficient number of timely blood Pb measurements (Fig. 1). Unlike in New York City for instance, infants are not systematically tested for blood Pb in France and their exposure before the fire is therefore also not well known.

Seven weeks after the cathedral fire, local authorities offered to test children from volunteer families, but the number of tests remained very low through July, 2019. After exposure ends, blood-Pb levels can decline within a few weeks although it can also take much longer (Barbosa et al., 2005). The low proportion (1%) of children reported with blood-Pb levels $>50 \mu\text{g}/\text{L}$ is welcome news but may mask a temporarily much higher level of exposure in the days to a few weeks after the fire. The few cases of surfaces elevated in Pb reported for schools in the affected area also date from summer 2019 and therefore likely underestimate peak exposure in the 1-2 weeks following the fire, especially if the schools had followed earlier recommendations and already cleaned the common areas. Finally, because the blood survey was relying on volunteers instead of proactively seeking all 6,000 potentially exposed children in the affected area through a door-

to-door survey, it was probably biased towards a more educated, wealthier segment of the population that may have been less at risk. In a post-coronavirus world, the need and feasibility of a testing campaign of the magnitude commensurate with the scale of a large fire or other environmental accident has become much harder to argue against.

5 Conclusions

A report issued by the ARS (2019h) on April 16, 2020, exactly one year after the fire, acknowledges the possibility that more people than indicated by the available data may have been exposed to Pb as a result of the cathedral fire. Our observations support this scenario. The soil data show that the levels of Pb contamination expressed in terms of mass per unit area documented within 100 m of the cathedral during summer 2019, several months after the fire, are comparable to the Pb fallout that extended downwind of the cathedral to a distance of 1 km. Therefore, elevated levels of Pb in indoor dust probably extended up to 1 km from the cathedral as well.

From a policy perspective, the tracking of the impact of Pb from the Notre-Dame fire suggests that the administration of large cities such as Paris should have a large environmental investigation team on standby, ready to be deployed to make hundreds of measurements immediately after an accident or toxic spill that could potentially pose a threat to public health. The city of Paris in fact has such a team (<http://laboratoirecentral.interieur.gouv.fr/Presentation/Le-LCPP/Panorama>), which was deployed and collected Pb data after the fire, but evidently not rapidly enough or at the required scale. The results from such an environmental investigation should be communicated immediately in ways that allow the general public to know exactly where the hazards are, which is very easy today using the mapping function of smartphones. In addition, public health authorities should be more prepared to survey immediately with environmental testing and biomarkers measurements by going door to door instead of waiting for volunteers and, again, rapidly communicate those results while providing the necessary privacy protection.

Acknowledgments

This project was supported in part by NIEHS P42 grant ES010349 and NSF grant CNS-1730414. A. Casella and C. van Geen participated in the soil sampling. B. Bostick, S. Chillrud, and B. Mailloux provided helpful suggestions for interpreting the soil data. Exchanges with A. Lefranc, R. Charvet, P. Glorennec, and P. Garnoussi in France pointed us to publicly available data and gave us a perspective of the activities conducted by French authorities in the aftermath of the fire. The entire data set and an interactive map of the test results with photos of each sampling site are available at <https://shorturl.at/kuvD5>, and the replication R and Stan code at <https://github.com/yao-yl/parisPb>. The data will also be made available through an approved repository upon acceptance.

Reference

- Agence Régionale de la Santé (2019a). <https://www.pressesante.com/wp-content/uploads/2019/04/CP-PP-27042019-Information-aux-riverains-de-Notre-Dame-1-3.pdf>
- Agence Régionale de la Santé (2019b). <https://www.iledefrance.ars.sante.fr/incendie-notre-dame-information-aux-riverains-sur-les-consequences-des-retombees-de-plomb>
- Agence Régionale de la Santé (2019c). <https://www.iledefrance.ars.sante.fr/suivi-des-recommandations-sanitaires-suite-lincendie-de-la-cathedrale-notre-dame-de-paris>

- Agence Régionale de la Santé (2019d). <https://www.iledefrance.ars.sante.fr/system/files/2019-07/DP-point-de-situation-Notre-Dame-de-Paris.0.pdf>
- Agence Régionale de la Santé (2019e). <https://www.iledefrance.ars.sante.fr/mise-au-point-de-lars-ile-de-france-suite-un-article-de-mediapart>
- Agence Régionale de la Santé (2019f). <https://www.iledefrance.ars.sante.fr/suivi-des-consequences-de-lincendie-de-notre-dame-point-de-situation-au-27112019>
- Agence Régionale de la Santé (2019g). https://www.iledefrance.ars.sante.fr/system/files/2019-10/PE.Plombemies_ND_10%2010%202019.pdf
- Agence Régionale de la Santé (2019h). <https://www.iledefrance.ars.sante.fr/incendie-de-notre-dame-de-paris-bilan-sanitaire-un>
- Aizer, A. & Currie, J. (2019). Lead and Juvenile Delinquency: New Evidence from Linked Birth, School and Juvenile Detention Records. *The Review of Economics and Statistics*, 101, 575-587.
- Alexievich, S. (2006) Voices from Chernobyl: The Oral History of a Nuclear Disaster, Picador, USA.
- ANSES (2020). La contamination d'espaces publics extérieurs par le plomb. Agence nationale de sécurité sanitaire de l'alimentation, de l'environnement et du travail. Saisine n° 2019-SA-0147. <https://www.anses.fr/fr/system/files/AIR2019SA0147.pdf>
- Barbosa Jr, F., Tanus-Santos, J. E., Gerlach, R. F., & Parsons, P. J. (2005). A critical review of biomarkers used for monitoring human exposure to lead: Advantages, limitations, and future needs. *Environmental Health Perspectives*, 113, 1669-1674.
- Brown, A., Franken, P., Bonner, S., Dolezal, N., & Moross, J. (2016). Safecast: successful citizen-science for radiation measurement and communication after Fukushima. *Journal of Radiological Protection*, 36,, S82-S101.
- Cheng, Z., Zheng, Y., Mortlock, R., & van Geen, A. (2004). Rapid multi-element analysis of groundwater by high-resolution inductively coupled plasma mass spectrometry. *Analytical and Bioanalytical Chemistry*, 379, 513-518.
- Chillrud, S. N., Bopp, R. F., Simpson, H. J., Ross, J. M., Shuster, E. L., Chaky, D. A., Walsh, D. C., Choy, C. C., Tolley, L. -R., & Yarme, A. (1999). Twentieth century atmospheric metal fluxes into Central Park Lake, New York. *Environmental Science & Technology*, 33, 657-662.
- Daly, C. (1866). La couverture de Notre-Dame de Paris. *Revue Générale de l'Architecture et des Travaux Publics*, 14, 211-212.
- Etchevers, A., Le Tertre, A., Lucas, J-P., Bretin, P., Oulhote, Y., Le Bot, B., & Glorenec, P. (2015). Environmental determinants of different blood lead levels in children: A quantile analysis from a nationwide survey. *Environment International*, 74, 152-159.
- Fowler, D., Skiba, U., Nemitz, E., Choubedar, F., Branford, D., Donovan R., & Rowland, P. (2004). Measuring Aerosol and Heavy Metal Deposition on Urban Woodland and Grass Using Inventories of 210Pb and Metal Concentrations in Soil. *Water, Air, & Soil Pollution: Focus* 4, 483-499.

- 495 Glorennec, P., Lucas, J.P., Mercat, A.C., Roudot, A.C., & Le Bot, B. (2016). Environ-
496 mental and dietary exposure of young children to inorganic trace elements. *Envi-*
497 *ronment international*, 97, 28-36.
- 498 HCSP (2014). Expositions au plomb: détermination de nouveaux objectifs de gestion.
499 Haut Conseil de la Santé Publique. www.hcsp.fr
- 500 JORF (2009). Arrêté du 12 mai 2009 relatif au contrôle des travaux en présence de plomb,
501 réalisés en application de l'article L. 1334-2 du code de la santé publique. Journal
502 Officiel de la République Française [https://www.legifrance.gouv.fr/affichTexte](https://www.legifrance.gouv.fr/affichTexte.do?cidTexte=JORFTEXT000020668963&categorieLien=id)
503 [.do?cidTexte=JORFTEXT000020668963&categorieLien=id](https://www.legifrance.gouv.fr/affichTexte.do?cidTexte=JORFTEXT000020668963&categorieLien=id)
- 504 Laidlaw M. A., & G. M. Filippelli, G. M. (2008). Resuspension of urban soils as a per-
505 sistent source of lead poisoning in children: A review and new directions. *Applied*
506 *Geochemistry*, 23, 2021-2039.
- 507 Landes, F., Paltseva, A., Sobolewski, J., Cheng, Z., Ellis, T., Mailloux, B., & van Geen,
508 A. (2019). A field procedure to screen soil for hazardous lead. *Analytical Chem-*
509 *istry*, 91, 8192-8198.
- 510 Lanphear B. P., Emond M., Jacobs D.E., Weitzman M., Tanner M., Winter N. L., Yakir
511 B., & Eberly S. (1995). A side-by-side comparison of dust collection methods for
512 sampling lead-contaminated house dust. *Environmental Research*, 68, 114-23.
- 513 Lanphear, B. P., Hornung, R., Khoury, J., Yolton, K., Baghurst, P., Bellinger, D. C., Can-
514 field, R.L., et al. (2005). Low-level environmental lead exposure and children's in-
515 tellectual function: an international pooled analysis. *Environmental Health Per-*
516 *spectives*, 113, 894-899.
- 517 Le Monde (2019). Après l'incendie de Notre-Dame, une plainte contre la pollution au
518 plomb. [https://www.lemonde.fr/planete/article/2019/07/29/pollution-au](https://www.lemonde.fr/planete/article/2019/07/29/pollution-au-plomb-autour-de-notre-dame-plainte-contre-x-pour-mise-en-danger-d-autrui_5494472_3244.html)
519 [-plomb-autour-de-notre-dame-plainte-contre-x-pour-mise-en-danger-d-autrui](https://www.lemonde.fr/planete/article/2019/07/29/pollution-au-plomb-autour-de-notre-dame-plainte-contre-x-pour-mise-en-danger-d-autrui_5494472_3244.html)
520 [_5494472_3244.html](https://www.lemonde.fr/planete/article/2019/07/29/pollution-au-plomb-autour-de-notre-dame-plainte-contre-x-pour-mise-en-danger-d-autrui_5494472_3244.html)
- 521 Mediapart (2019). Notre-Dame: des taux de plomb chez les enfants supérieurs au seuil
522 de vigilance. [https://www.mediapart.fr/journal/france/050819/notre-dame](https://www.mediapart.fr/journal/france/050819/notre-dame-des-taux-de-plomb-chez-les-enfants-superieurs-au-seuil-de-vigilance?onglet=full)
523 [-des-taux-de-plomb-chez-les-enfants-superieurs-au-seuil-de-vigilance](https://www.mediapart.fr/journal/france/050819/notre-dame-des-taux-de-plomb-chez-les-enfants-superieurs-au-seuil-de-vigilance?onglet=full)
524 [?onglet=full](https://www.mediapart.fr/journal/france/050819/notre-dame-des-taux-de-plomb-chez-les-enfants-superieurs-au-seuil-de-vigilance?onglet=full)
- 525 Miquel, G. (2001). Rapport sur les effets des métaux lourds sur l'environnement et la
526 santé. Office parlementaire d'évaluation des choix scientifiques et technologiques.
527 French Senate report. <https://www.senat.fr/rap/100-261/100-26150.html>
- 528 Motelay-Massei, A., Ollivon, D., Tiphagne, K., & B. Garban, B. (2005). Atmospheric
529 bulk deposition of trace metals to the Seine river Basin, France: concentrations,
530 sources and evolution from 1988 to 2001 in Paris. *Water Air Soil Pollut*, 164, 119-135.
- 531 Robin des Bois (2019). Ile de la Cité: a new polluted site in Paris. [https://robindesbois](https://robindesbois.org/notre-dame-un-nouveau-site-pollue-a-paris/)
532 [.org/notre-dame-un-nouveau-site-pollue-a-paris/](https://robindesbois.org/notre-dame-un-nouveau-site-pollue-a-paris/)
- 533 Selim, H. M. (2017). Competitive Sorption and Transport of Heavy Metals in Soils and
534 Geological Media. CRC Press, Boca Raton, Florida, USA.
- 535 Stan Development Team (2018). Stan Modeling Language Users Guide and Reference
536 Manual, Version 2.18.0. <http://mc-stan.org>